

Isomeric Product Distributions from the Self-Reaction of Propargyl Radicals

Weiyong Tang, Robert S. Tranter,[†] and Kenneth Brezinsky*

Departments of Mechanical Engineering and Chemical Engineering, University of Illinois at Chicago, 842 West Taylor Street, M/C 251, Chicago, Illinois, 60607

Received: February 4, 2005; In Final Form: April 4, 2005

We have investigated the isomeric C₆H₆ product distributions of the self-reaction of propargyl (C₃H₃) radicals at two nominal pressures of 25 and 50 bar over the temperature range 720–1350 K. Experiments were performed using propargyl iodide as the radical precursor in a high-pressure single-pulse shock tube with a residence time of 1.6–2.0 ms. The relative yields of the C₆H₆ products are strongly temperature dependent, and the main products are 1,5-hexadiyne (15HD), 1,2-hexadiene-5-yne (12HD5Y), 3,4-dimethylenecyclobutene (34DMCB), 2-ethynyl-1,3-butadiene (2E13BD), fulvene, and benzene, with the minor products being *cis*- and *trans*-1,3-hexadiene-5-yne (13HD5Y). 1,2,4,5-Hexatetraene (1245HT) was observed below 750 K but the concentrations were too low to be quantified. The experimentally determined entry branching ratios are: 44% 15HD, 38% 12HD5Y, and 18% 1245HT, which is efficiently converted to 34DMCB. Following the initial recombination step, various C₆H₆ isomers are formed by thermal rearrangement. The experimentally observed concentrations for the C₆H₆ species are in good agreement with earlier experiments on 15HD thermal rearrangement.

Introduction

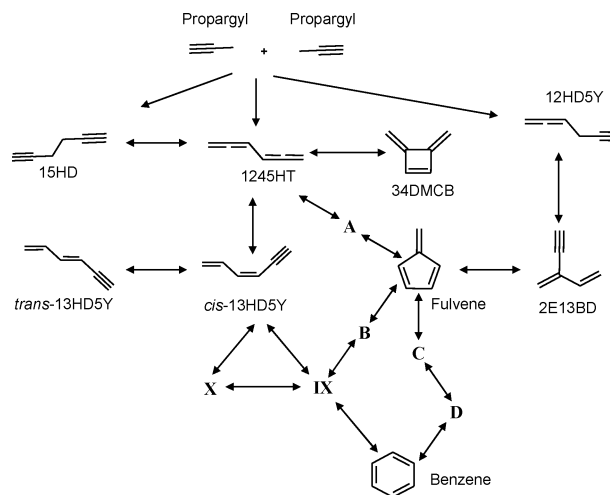
The formation of the first aromatic ring from small radicals and molecules present in flames is an important aspect of developing mechanisms for the production of larger polyaromatic systems. Currently, the self-reaction of propargyl (C₃H₃) radicals, R1



is generally thought to be one of the most important reactions forming benzene^{1–6} due to its relatively high concentrations in oxidizing environments. The formation of benzene from propargyl radicals is not a simple process as it is sometimes represented in various aromatic kinetic models^{7–10} where one or two global reactions represent C₃H₃ recombination chemistry. Instead the reaction occurs on a complex multichannel potential-energy surface (PES) that begins with the simultaneous production of three linear C₆H₆ isomers (1,5-hexadiyne (15HD), 1,2,4,5-hexatetraene (1245HT), and 1,2-hexadiene-5-yne (12HD5Y), see Scheme 1 for structures) that are formed from the various head/tail combinations of propargyl radicals. These initial products then isomerize through several other configurations to ultimately form benzene. If the reaction temperature is sufficiently high, then the benzene will dissociate to form a phenyl radical and a hydrogen atom.

Several groups^{11–18} have tackled the problem of calculating an accurate PES for the complex C₃H₃ + C₃H₃ reaction, and the most sophisticated of these was published by Miller and Klippenstein¹⁸ in late 2003. This work refined a PES from earlier BAC-MP4 calculations^{12,13} and included a path that connected 1245HT to 1,3-hexadiene-5-yne (13HD5Y), which then goes on to benzene without passing through fulvene thereby characterizing an alternate route to benzene that appeared warranted based on earlier experimental studies.¹⁹ By use of a Rice–

SCHEME 1: Chemical Reaction Pathways of the Recombination of Propargyl Radicals and Subsequent C₆H₆ Isomerization^a



^a The length of the arrow does not indicate the significance of the path. X, IX, A, B, C, and D are highly reactive C₆H₆ intermediates. Refer to ref 18 for detailed energy levels and structures of X, IX, and A–D.

Ramsperger–Kassel–Marcus (RRKM)-based master equation approach and the new PES, Miller and Klippenstein could accurately simulate the product distributions of low-temperature flow reactor 15HD pyrolysis by Stein and co-workers.¹⁹ Scheme 1 presents the main reaction paths involved on the PES of Miller and Klippenstein to convert propargyl radicals into benzene, and the reader is referred to ref 18 for a detailed energy-level diagram.

The first experimental study on reaction R1 was conducted by Alkemade and Homann using a low-pressure flow reactor (LPFR) coupled via a nozzle/skimmer arrangement to a mass spectrometer (MS).²⁰ Since then, several investigations have been conducted employing a variety of techniques and radical

* To whom correspondence should be addressed. E-mail: kenbrez@uic.edu.

[†] Current address: Chemistry Division, Argonne National Laboratory, Argonne, IL, 60439.

TABLE 1: Experimental Determination of the Overall Recombination Rate Constant of $C_3H_3 + C_3H_3 \rightarrow$ Products, Listed Chronologically in Order of Publication

$k/10^{-11} \text{ cm}^3 \text{ molecule}^{-1} \text{ s}^{-1}$	T/K	P/bar	method	ref
5.7	623, 673	3, 6 mbar	LPFR/MS	20(1989)
1.2 ± 0.2	295	20 mbar	laser photolysis/IR absorption	21(1994)
4.3 ± 0.6	295	3, 133 mbar	laser photolysis/cavity ring-down spectroscopy	22(1999)
4.0 ± 0.4	295	67 mbar	laser photolysis/GC/MS	23(2000)
1.24	1100–2100	1.5–2.2 bar	shock tube/ARAS	24(2000)
3.9 ± 0.6	296	8 mbar	laser photolysis/IR absorption	25(2003)
$3.3-1.2$	500–1000	2–8 mbar	laser photolysis/MS	26(2003)
$2.4-4.1$	373–520	1–140 bar	laser photolysis/UV absorption	27(2003)
$\sim 0.8-1.5$	995–1440	0.6–1.0 bar	shock tube/UV absorption	28(2004)
0.22	1400 ± 50	27 mbar	fitted to flame measurements	29(2004)

TABLE 2: Experimental Observation of the Isomeric C_6H_6 Products of the $C_3H_3 + C_3H_3$ Reaction, Listed Chronologically in Order of Publication^a

T/K	P	t	15HD	1245HT	34DMCB	fulvene	12HD5Y	2E13BD	<i>cis</i> -13HD5Y	<i>trans</i> -13HD5Y	benzene	ref
623, 673	3, 6 mbar	4.0 ms	✓	✓			✓		✓ ^b	✓ ^b	✓	20
295	67 mbar	1.0–2.0 s ^c	✓				✓					23
1100–2100	1.5–2.2 bar	~ 1.0 ms	✓								✓	24
500–1000	2–8 mbar	120 ms	✓			×					✓	26
295–623	3, 133 mbar	1.0–2.0 s ^c	✓		✓	×	✓				✓	30
720–1350	25 bar, 50 bar	1.6–2.0 ms	✓	×	✓	✓	✓	✓	×	×	✓	p.w.

^a Note: × represents compound with a yield <10%. ✓ represents compound with a yield >10%. ^b Trans and cis structures were not resolved. ^c Multiple laser shots averaged in this period. ^d Too low to be quantified.

sources^{21–30} with the majority of these experiments determining only the overall recombination rate^{20–29} and only a few studies giving detailed product distributions. In addition to the direct measurements, an “optimized” recombination rate obtained by fitting a detailed kinetic model to fuel-rich acetylene flame measurements²⁹ at 1400 K and 20 torr was also reported. As can be seen in Table 1, reasonable agreement has been achieved between the different studies with the total recombination rate lying in the range $0.22-5.7 \times 10^{-11} \text{ cm}^3 \text{ molecule}^{-1} \text{ s}^{-1}$ from 295 to 2100 K and 2 mbar to 140 bar. Moreover, the experimentally determined overall recombination rate coefficients are predicted well by the theoretical work of Miller and Klippenstein.¹⁸

In contrast to the relatively large number of studies determining recombination rate coefficients, there are only some limited literature data containing detailed product analyses for propargyl recombination. In their flow-reactor work, Alkemade and Homann²⁰ obtained product yields at temperatures of 623 and 673 K and at pressures of 3 and 6 mbar with a retention time of 4 ms. The product distributions were strongly influenced by temperature and pressure, and the reported ranges for each species are shown in parentheses: 15HD (2–11%), 12HD5Y (30–46%), 1245HT (7–19%), 13HD5Y (15–19%), and benzene (19–30%). At 500–1000 K and 2–8 mbar, which spans Alkemade–Homann’s conditions, a flow tube study by Schafir et al.²⁶ positively identified 15HD, benzene, and fulvene and observed two additional C_6H_6 isomers that could not be identified. 3,4-Dimethylenecyclobutene (34DMCB) was not detected in either study. Fahr and Nayak²⁴ reported the recombination yields at 295 K and 50 torr to be 60% 15HD, 25% 12HD5Y, and 15% of another unidentified C_6H_6 species. Two more C_6H_6 isomers, 34DMCB and fulvene, were identified in subsequent work conducted in the same laboratory by Howe and Fahr.³⁰ Finally Scherer et al.²⁴ analyzed post shock samples, $1100 < T < 2100$ K and $1.5 < P < 2.2$ bar, from a shock tube that was not optimized as a single-pulse apparatus by gas chromatography (GC)/mass spectrometry (MS) and GC/flame ionization detection (FID). At their lowest reaction temperatures, Scherer et al. observed eight baseline resolved peaks all with the molecular formula C_6H_6 and they were able to positively identify only 15HD and benzene. The species identified in the

various experimental studies are summarized in Table 2 where only positively identified products are included.

The theoretical work by Miller and Klippenstein¹⁸ is able to give reasonable predictions of Fahr and Nayak’s species profiles²³ but shows disagreement with the Alkemade–Homann work²⁰ for which the simulation is good only for benzene and 13HD5Y. In particular, the calculations greatly underpredict the experimental [1245HT] (<5%). Furthermore, the theory predicts a considerable amount of fulvene ($\sim 18\%$) and 2-ethynyl-1,3-butadiene (2E13BD) ($\sim 26\%$), species that were not detected by Alkemade and Homann. Of additional importance, Alkemade and Homann are the only group to have observed 1245HT as a direct reaction product and it is formed in significant quantities.

Clearly there is some degree of discrepancy between theory and experiment in terms of the isomeric product distribution, and to further understand propargyl recombination, more experimental data are required. One impediment to performing experiments is the difficulty of unambiguously identifying the C_6H_6 products formed during propargyl recombination and their subsequent isomeric counterparts. This challenge has been addressed recently in a shock-tube study of 15HD thermal rearrangement^{31,32} where a novel technique, GC-matrix isolation-Fourier transform IR-MS (GC-MI-FTIR-MS), was used to obtain simultaneous mass and FTIR spectra for species eluting from the GC column.³¹ The FTIR spectra were used to positively identify all of the stable species predicted by Miller and Klippenstein, as shown in Scheme 1, except 1245HT, which was not present in the samples analyzed. Among them, *cis*- and *trans*-13HD5Y were detected for the first time. Thus an experimental investigation of propargyl recombination in the high-pressure shock tube can build on the experience gained with 15HD to obtain detailed product profiles from which branching ratios for various channels and rate coefficients can be obtained.

Experimental Section

1. Shock-Tube Apparatus. The experiments were performed in the UIC high-pressure single-pulse shock tube (HPST) which is described in detail elsewhere,^{33,34} and only a brief description will be given here. The HPST consists of a 1 in. inside diameter

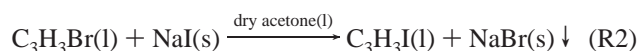
(i.d.) driven section and a 2 in. i.d. driver section and can be operated up to reflected shock pressures, P_5 , of 1000 bar, although in this work the P_5 values were constrained to 25 and 50 bar. A dump tank is situated just downstream of the diaphragm section and quenches the reflected shock wave thereby preventing multiple heating events occurring during an experiment. Samples of the quenched gases are withdrawn via a port in the endwall of the driven section for offline analysis along with a sample of the reagent mixture that was taken from the shock tube immediately before firing the HPST. Prior to each experiment, the driven section of the shock tube was evacuated to at least 1×10^{-5} Torr with a turbo-pump/rotary-oil-pump combination.

Shock waves are generated by spontaneously bursting prescored diaphragms between the driver and driven sections of the shock tube, and the reactions take place in the stable, isothermal zone behind the reflected shock waves close to the endwall of the driven section. These experiments were performed at nominal pressures of 25 and 50 bar using aluminum diaphragms of 0.025 in./0.010 in. (thickness/score depth) and 0.025 in./0.005 in., respectively. As is normal in shock-tube experiments the actual reaction pressures span a small range encompassing the nominal pressures. The actual reaction pressures for each experiment are used in simulations and are available in the Supporting Information.

For each experiment, the reaction pressure, P_5 , reaction temperature, T_5 , and reaction time, t , were obtained. Pressures behind the reflected shock wave and reaction times were obtained from the pressure profiles measured by a piezoelectric pressure transducer (PCB Model No. 113A23) mounted axially in the endwall of the driven section. The reaction time of each experiment was measured from the arrival of the incident shock wave at the end wall of the driven section to the observed pressure at the end wall falling to 80% of its maximum.³⁵ The reaction times in the current work were in the range of 1.6–2.0 ms. The reaction temperatures were calculated from the incident shock velocity and errors in the temperature due to deviations from ideal gas behavior are expected to be small for these reaction pressures.³⁶ Shock velocities were calculated from the time taken for the incident shock wave to travel between piezoelectric pressure transducers mounted along the side wall near the end wall of the driven section of the shock tube.

For each experiment, a sample of the reagent gas was taken prior to firing the shock tube, preshock sample, and a sample of the gas near the endwall of the driven section of the shock tube was collected shortly after the arrival of the expansion wave generated from bursting the diaphragm, postshock sample. Both the preshock and postshock samples are collected in electropolished stainless steel vessels which were stored in an oven at 45 °C prior to analysis by gas chromatography. For all experiments, the samples were analyzed within 3 h of collection to minimize the possibility of degradation of the samples particularly via the slow isomerization of propargyl iodide to iodoallene.

2. Preparation of Propargyl Iodide. In the current work, propargyl iodide was used as the precursor for propargyl radicals and was synthesized via the Finkelstein reaction³⁷ as shown in R2



The procedure for synthesizing $\text{C}_3\text{H}_3\text{I}$ is as follows. A 200-mL portion of dry acetone (Aldrich, 99.5+%) was saturated with 35 g of sodium iodide (Aldrich, 99+%). The saturated

solution was then decanted, and 11 mL of propargyl bromide ($\text{C}_3\text{H}_3\text{Br}$, TCI America, 97+%) were added to the NaI solution and shaken. A precipitate is immediately formed. NaBr, the solid product, is insoluble in acetone but very soluble in water, and the precipitate was removed by washing with distilled water. The aqueous and organic phases were allowed to separate in a separating funnel, and then the organic phase was washed several more times with water. Normally, a few milliliters of the organic phase could be collected after the washing procedure. Finally, a low-temperature (approximately -30 °C) vacuum distillation was performed to remove the remaining acetone and water and the purified $\text{C}_3\text{H}_3\text{I}$ was stored over a few crystals of anhydrous sodium sulfate (Lancaster, 98+%) in a refrigerator. GC/MS analysis was used to determine the purity of $\text{C}_3\text{H}_3\text{I}$, and typically the final product was 99.5+% $\text{C}_3\text{H}_3\text{I}$. The analytical method revealed that both propargyl iodide and iodoallene were present in the final product although no bromoallene was found in the starting materials. The identities of the two isomers were determined by GC/MS and $[\text{P}-\text{C}_3\text{H}_3\text{I}]_0/[\text{A}-\text{C}_3\text{H}_3\text{I}]_0 \approx 15/1$, where P and A stand for the propargyl iodide and iodoallene, respectively. Typically $\text{C}_3\text{H}_3\text{I}$ was used to prepare reagent mixtures on the same day it was prepared, as over the course of a few weeks there is a slow isomerization from the P to A forms of $\text{C}_3\text{H}_3\text{I}$.

3. Reagent Mixtures. The reagent mixtures were prepared manometrically in 50-L high-pressure vessels and allowed to stand overnight before use. The mixtures contained 40–65 ppm $\text{C}_3\text{H}_3\text{I}$, 2500 ppm neon (AGA, 99.99%) with the balance argon (BOC, 99.999%). The argon was passed over Oxisorb (Messer-Griesheim) to remove traces of O_2 prior to admission to the mixing vessel, and neon was used as supplied. Neon is used as an internal standard for the analytical work and to account for any dilution of the postshock sample by the driver gas, He (BOC, 99.9%). In the 15HD experiments the mixing vessel was maintained at 45 °C. However, in the present work the tank was kept at room temperature (approximately 25 °C) to minimize isomerization of propargyl iodide to iodoallene and under these conditions the reagent mixtures were stable for several days.

4. Analytical Technique. A similar methodology to that employed in the isomerization of 1,5-hexadiyne experiments^{31,32} was used in the present work with minor modifications to allow propargyl iodide and iodoallene to be detected along with the C_6H_6 isomers. The bulk of the analyses were performed using an Agilent Model 6890 gas chromatograph equipped with a HP-Molseive5A column (30 m, 0.32 mm, 12 μm) and a HP-1MS column (30 m, 0.32 mm, 3 μm). The HP-1MS column eluted to a FID and the HP-Molseive5A eluted to a TCD. Gas sample valves were used to admit samples to the columns and the sampling loops on each valve were filled simultaneously from the sample vessels via a vacuum rig. To improve the separation, H_2 was used as the carrier gas.

Nine C_6H_6 isomers in addition to the parent molecules propargyl iodide and iodoallene were detected and baseline resolved. On the basis of our prior work with 15HD, the identification of the majority of the species detected was straightforward. In addition, 1245HT, which had not been detected in the earlier 15HD work³¹ but is a potential product in the current work, was synthesized by the method of Hopf and co-workers.^{38,39} GC-MI-FTIR-MS was used to confirm the identity of the 1245HT. Its elution order relative to the other C_6H_6 isomers from the HP1-MS column was obtained. In addition, in the present study the Kovats indices of C_6H_6 compounds were calculated. The Kovats retention index is a

TABLE 3: Kovats Index of C₆H₆ Species Detected in This Work

C ₆ H ₆ species	present work ^a	Alkemade and Homann ^b
2E13BD	601.5	
15HD	612.1	616
34DMCB	620.4	
fulvene	624.9	
<i>cis</i> -13HD5Y	629.8	626
<i>trans</i> -13HD5Y	636.1	626
benzene	644.8	647
12HD5Y	648.5	656
1245HT	697.1	698

^a 1-Heptane and 1-pentane were used as reference compounds.

^b *trans*- and *cis*-13HD5Y structures were not resolved.

logarithmic scale on which the adjusted retention time of a peak is compared with those of linear *n*-alkanes as reference compounds. The Kovats retention index system is an accurate method for reporting gas chromatographic data for inter-laboratory substance identification. Table 3 compares the present result with previously reported by Alkemade and Homann.²⁰

Where possible authentic standards were used to calibrate the detector response for different species with the following exceptions. The concentrations of propargyl iodide and iodoallene were determined with the assumption of identical response properties under current GC conditions. The calibration coefficient for benzene was applied to fulvene and 34DMCB, and the calibration coefficient for 15HD was used for the other linear C₆H₆ species.

Previously, Scherer et al.²⁶ used a Poraplot-Q column in the GC/MS analysis of their postshock samples. They observed eight C₆H₆ species with baseline resolution of which they were able to identify only 15HD and benzene. Both 15HD and benzene appear in the same elution order relative to the other species as is observed in this work, and it is likely that the elution order for the HP-1MS column and the Poraplot-Q columns are the same for the various C₆H₆ isomers which are listed in Table 2.

Figure 1 displays two typical GC/FID analytical chromatograms of postshock samples with one obtained at $T_5 = 844$ K and the other at $T_5 = 1074$ K. Besides the parent molecules, P-C₃H₃I and A-C₃H₃I, nine isomeric C₆H₆ products were detected and identified, of which all were quantified with the exception of 1245HT. Trace amounts of 1245HT were observed for $T_5 < 750$ K but the concentration was too low to be quantitatively measured.

Results

More than 100 experiments were performed covering the temperature range 720–1350 K to map out the product distributions of the C₃H₃ + C₃H₃ reaction at two nominal pressures of 25 and 50 bar. At each pressure, two different reagent mixtures were used with initial C₃H₃I concentrations of 40 and 60 ppm for the 25 bar experiments and 55 and 65 ppm for the 50 bar experiments, respectively. At $T_5 = 720$ K, C₃H₃I starts to decompose to C₃H₃ radicals (~5%), and at $T_5 = 1340$ K benzene is the dominant product (~90%).

The distributions of residual C₃H₃I and total C₆H₆ production in the postshock sample as a function of temperature at 25 bar and at 50 bar are shown in Figures 2 and 3, respectively. Also shown in the inset figures of Figures 2 and 3 are the percentages of P-C₃H₃I and A-C₃H₃I. At 720 K, the [P-C₃H₃I]/[A-C₃H₃I] ratio in the postshock sample (1.7:1) is much smaller than that in the preshock sample (15:1). As the reaction temperature increases, [P-C₃H₃I] always decreases, while [A-C₃H₃I] increases until 800 K and then starts to decrease.

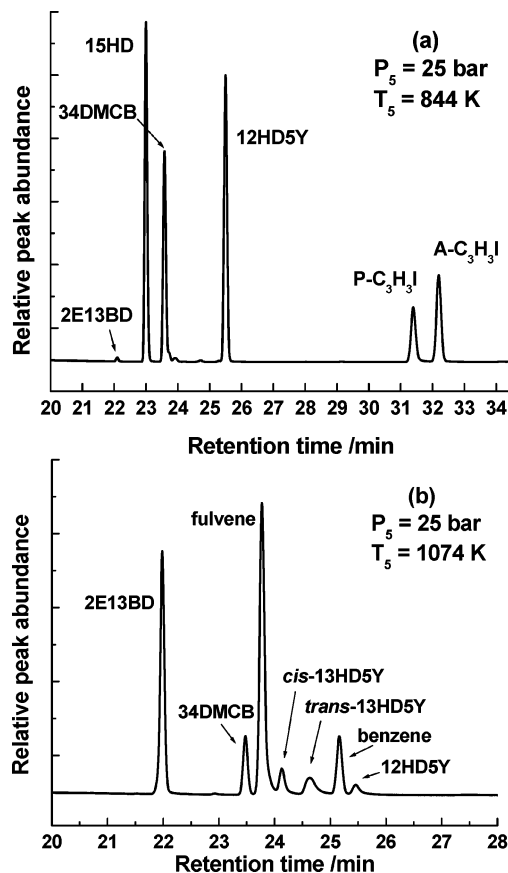


Figure 1. Gas chromatograms of two postshock samples from C₃H₃I pyrolysis at (a) 844 K and (b) 1074 K. Experiments were performed at 25 bar with [C₃H₃I]₀ = 40 ppm. 1245HT elutes with a RT = 29.2 min and it could only be observed when $T_5 < 750$ K.

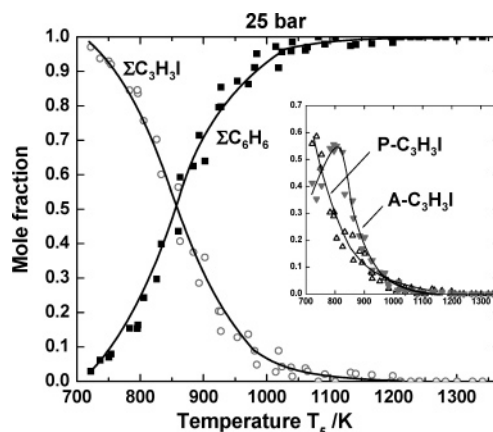


Figure 2. Product distributions of C₃H₃I and Σ C₆H₆ as a function of temperature at 25 bar in C₃H₃I pyrolysis ([P-C₃H₃I]₀/[A-C₃H₃I]₀ = 15/1). Reaction time ranged from 1.6 to 2.0 ms. Note the smooth curves were drawn only for visualization.

Over the complete temperature range of the experiments, the total amount of C₃H₃I always decreases. At $T_5 = 1000$ K, more than 95% of the initial C₃H₃I has been consumed, and the only products are various C₆H₆ isomers.

The distributions of the C₆H₆ isomers in the postshock samples are shown in Figures 4 and 5 as a function of temperature at 25 and 50 bar, respectively. Below 800 K, 15HD, 12HD5Y, and 34DMCB are the only products and are formed in an almost constant ratio of 2.4:2.1:1. 1245HT, the third direct linear combination product of C₃H₃, is not observed in quantifi-

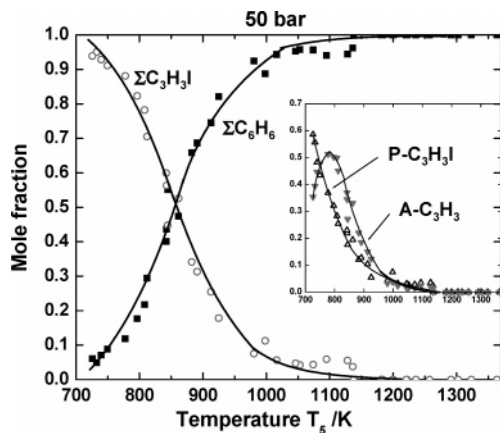


Figure 3. Product distributions of C_3H_3I and ΣC_6H_6 as a function of temperature at 50 bar in C_3H_3I pyrolysis ($[P-C_3H_3I]_0/[A-C_3H_3I]_0 = 15/1$). Reaction time ranged from 1.6 to 2.0 ms. Note the smooth curves were drawn only for visualization.

able amounts although as mentioned previously a trace amount of 1245HT is observed at the lowest reaction temperatures. As the reaction temperature increases from 800 to 900 K, the [15HD]:[34DMCB] ratio shifts to 0.2:1 while the observed concentration of 12HD5Y is barely changed. Above about 920 K very little 15HD remains in the postshock samples, and the concentration of 12HD5Y starts to decrease. The 34DMCB concentration reaches a maximum around 950 K.

For $T_5 < 900$ K, 15HD, 12HD5Y, and 34DMCB are the only products; however at 900 K, fulvene, 2E13BD, *cis*-13HD5Y, and *trans*-13HD5Y are formed. Benzene first appears when T_5 is approximately 1020 K and the minor products, *cis*- and *trans*-13HD5Y, reach maximum concentrations, at around 1060 K. Above about 1200 K, benzene is the only major product in the postshock samples that increases in concentration. All other products decrease until at around 1350 K fulvene and 2E13BD are the only species other than benzene present.

The effect of P_5 on the relative concentrations of species present in the postshock samples has been examined, and examples for C_3H_3I and 34DMCB are shown in Figures 6 and 7. The lack of pressure dependency at these high P_5 values is also displayed by the other species and is consistent with earlier work on 15HD isomerization in the HPST.³²

In the current work, the carbon balance was monitored for each test and Figure 8 displays the 50-bar shock carbon balance. The carbon balances show considerable scatter over the whole temperature range which cannot be attributed to the formation of heavy, nonvolatile species during the course of the reaction since no wall deposits were observed in the shock tube, cf. Shafir et al.²⁶ Currently the source of the scatter is not clear although it is potentially due to the GC rig and mixture tanks being unheated which was necessary to prevent degradation of the reagent mixture.

Discussion

1. Propargyl Iodide Decomposition and Isomerization. The majority of studies on propargyl recombination in the literature have used a halogenated propargyl (C_3H_3X , $X = Cl, Br,$ and I) as the C_3H_3 precursor.^{21–25,28,30,40} In general C_3H_3Cl and C_3H_3Br have been used in photolytic sources although one shock-tube study⁴⁰ employed C_3H_3Br as a thermal source. C_3H_3I has been used as a thermal source in two shock-tube studies.^{24,28}

For propargyl halides, the decomposition via R3 is in competition with the molecular elimination channel, R4, and

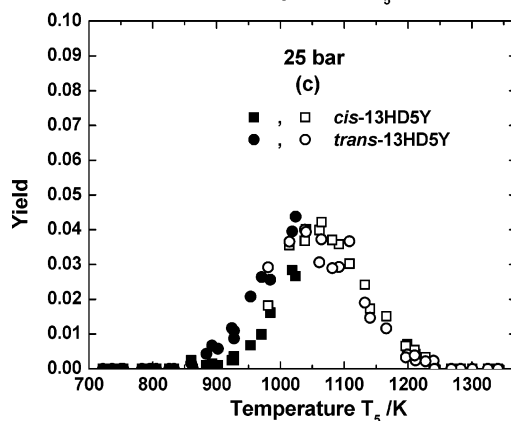
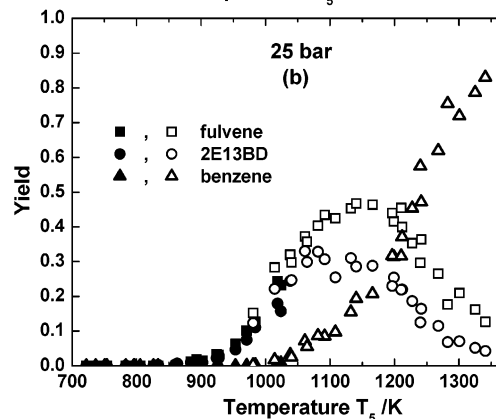
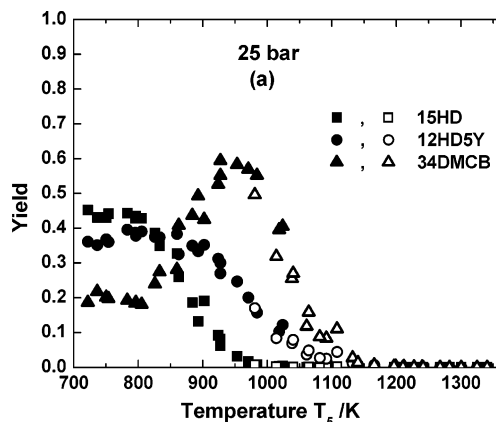
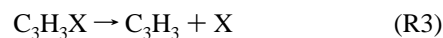


Figure 4. Relative yields of isomeric C_6H_6 as a function of temperature at 25 bar. Closed symbols, $[C_3H_3I]_0 = 40$ ppm; open symbols, $[C_3H_3I]_0 = 60$ ppm. In both mixtures, $[P-C_3H_3I]_0/[A-C_3H_3I]_0 = 15/1$.

for the chloride and bromide R4 can be significant^{41–43} thereby opening up additional reaction channels forming C_3H_2 .



C_3H_3I , by contrast, appears to be a much cleaner source most probably due to the weak C–I bond. Previous shock-tube/ARAS experiments by Scherer et al.²⁴ showed no evidence for R4 occurring at 1100–2100 K and 1.5–2.2 bar which was confirmed by Fernandez et al.²⁸ To assess the magnitude of R4 in the current work, a series of experiments were performed in which H_2 was added to the reagent mixture in a manner similar to earlier experiments with C_3H_3Br by Kern et al.⁴⁰ Recent work by Miller and Klippenstein⁴⁴ indicates that for the experimental conditions in the present study H_2 and C_3H_2 should react via R5 quickly and the excited C_3H_4 adduct should be stabilized

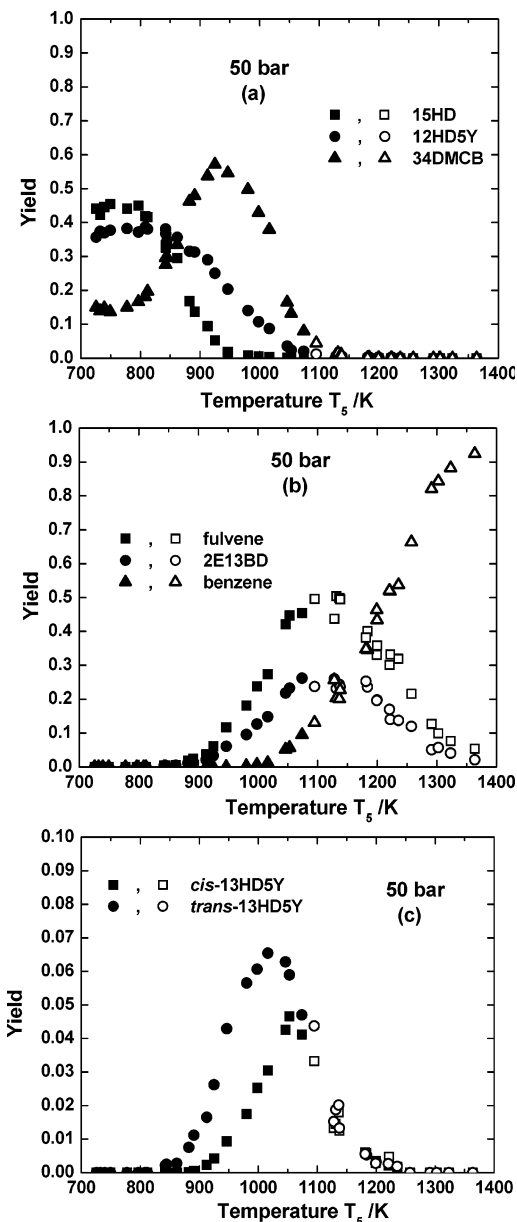


Figure 5. Relative yields of isomeric C_6H_6 as a function of temperature at 50 bar. Closed symbols, $[C_3H_3I]_0 = 55$ ppm; open symbols, $[C_3H_3I]_0 = 65$ ppm. In both mixtures, $[P-C_3H_3I]_0/[A-C_3H_3I]_0 = 15/1$.

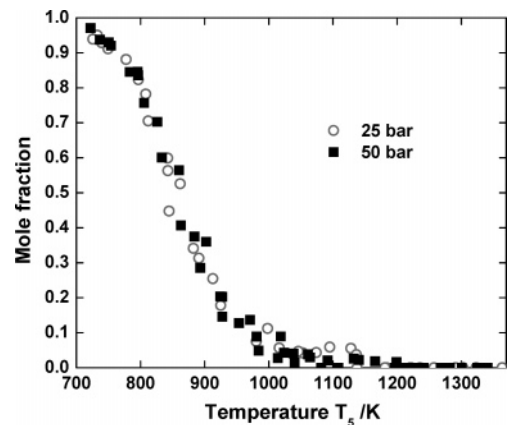


Figure 6. Effect of reaction pressure on C_3H_3I consumption.

via collisions with the bath gas to yield allene and propyne. Around a dozen experiments were performed using a reagent mixture with H_2 in addition to C_3H_3I ($[H_2]_0 = 60$ ppm and

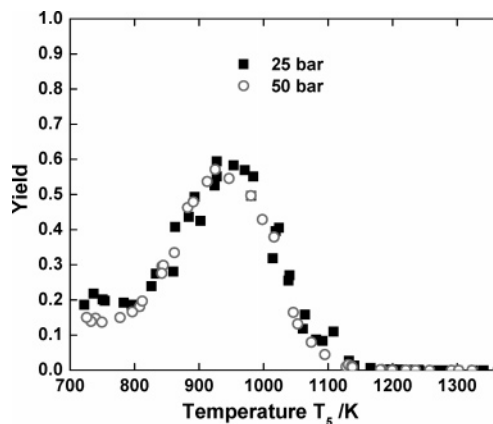


Figure 7. Effect of reaction pressure on the product yield of 34DMCB.

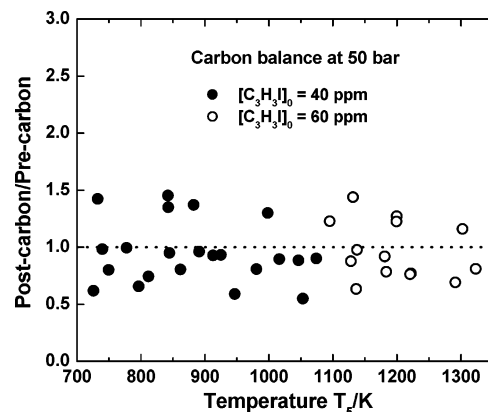


Figure 8. Carbon balance at 50 bar.

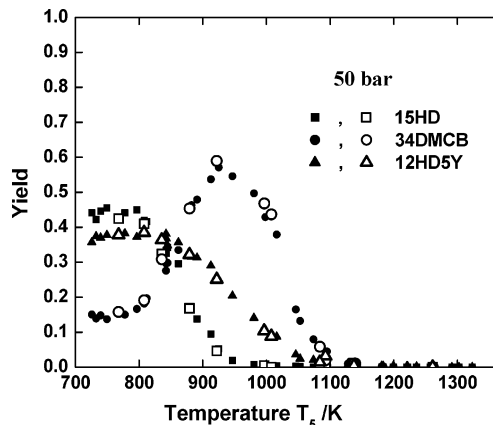
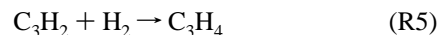


Figure 9. Comparison of the relative yields of isomeric C_6H_6 species with and without hydrogen addition in C_3H_3I at 50 bar. Closed symbols, without hydrogen addition; open symbols, with hydrogen addition of $[H_2]_0/[C_3H_3I]_0 = 1/1$ (vol). The same trends were found for other C_6H_6 species.

$[C_3H_3I]_0 = 60$ ppm) at 50 bar covering the temperature range of 720–1350 K. Neither of the C_3H_4 isomers was detected by GC/FID/MS analysis of the postshock samples from these experiments, a result that is consistent with the work by Scherer et al.²⁴ Additionally the C_6H_6 profiles were not perturbed by the addition of H_2 as shown in Figure 9.



Analyses of the freshly synthesized C_3H_3I clearly showed a small amount, about 6%, of iodoallene was formed along with propargyl iodide, and Figures 2 and 3 indicate that there is some

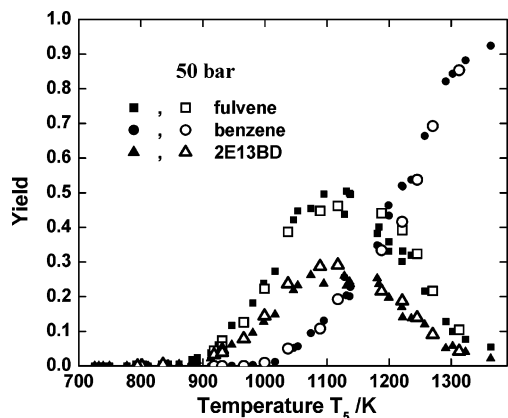


Figure 10. The effect of iodoallene presence on the relative yields of isomeric C_6H_6 species at 50 bar. Closed symbols, $[P-C_3H_3I]_0/[A-C_3H_3I]_0 = 15/1$; open symbols, $[P-C_3H_3I]_0/[A-C_3H_3I]_0 = 2/1$. The same trends were found for other C_6H_6 species.

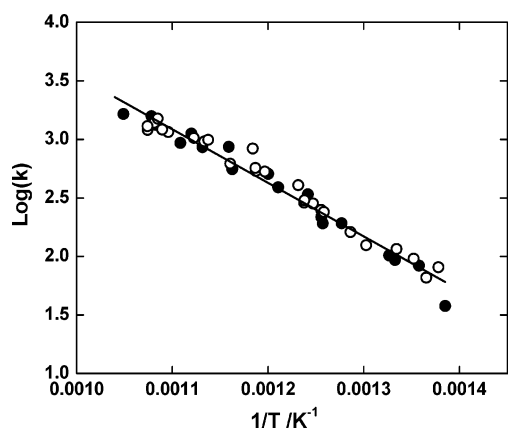
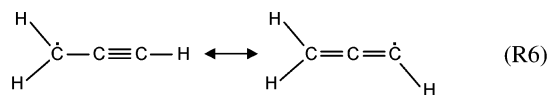


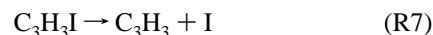
Figure 11. Arrhenius plot of the dissociation reaction $C_3H_3I \rightarrow C_3H_3 + I$. The solid line is the least-squares fit given in text. Closed symbols, 25 bar data; open symbols, 50 bar data. Note the isomerization between $P-C_3H_3I$ and $A-C_3H_3I$ is in parallel with the dissociation. See text for detailed discussion.

isomerization of $P-C_3H_3I$ to $A-C_3H_3I$ that occurs in parallel with the dissociation of C_3H_3I at low reaction temperatures. The $A-C_3H_3I$ will dissociate to form allenyl radicals which rapidly isomerize to form propargyl radicals, R6, which Miller and Klippenstein¹¹ suggest will be the dominant structure. If the experimental product distributions are sensitive to the $[P-C_3H_3I]_0/[A-C_3H_3I]_0$ ratio, then the initial $[A-C_3H_3I]$ needs to be accounted for in interpreting the results. Consequently, a reaction mixture was prepared with a much smaller ratio of $[P-C_3H_3I]_0/[A-C_3H_3I]_0 = 2/1$ than normally used (obtained simply by keeping the freshly synthesized propargyl iodide in a refrigerator for two months) and several experiments were performed at 50 bar over 720–1350 K. The results of these experiments are compared with the $[P-C_3H_3I]_0/[A-C_3H_3I]_0 = 15/1$ experiments at 50 bar in Figure 10, and clearly there is no difference between the two sets.



A rate coefficient of $k_7 = 10^{8.12} \times \exp(-20.9 \text{ Kcal}/RT)$ was estimated from the overall decomposition of C_3H_3I in the experimental results, Figure 11. In fact the estimated k_7 appears to be considerably smaller than that of Scherer et al.,²⁴ which was obtained by I-atom ARAS which indicated that for $T_5 >$

1000 K C_3H_3I dissociates effectively instantaneously. In the current work reaction times are on the order of 1.6–2.0 ms, and with the deduced k_7 C_3H_3I is not completely consumed (>99.9%) until 1200 K. However at the lower temperatures, $T_5 < 1000$ K, one has to bear in mind that reaction R7 is in competition with the isomerization reaction. The mechanism for the isomerization is not yet understood, and a series of experiments and theoretical calculations are currently being performed to address this problem. In this work the estimated k_7 is used to simulate the overall decomposition of C_3H_3I .

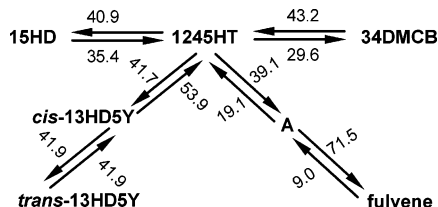


Under the conditions of the current work, I atoms produced in pyrolysis of the C_3H_3I should be effectively inert and predominantly combine with each other to form iodine molecules, cf. the production of H atoms via the decomposition of C_2H_5I behind reflected shock waves of Herzler and Frank⁴⁶ and the work of Scherer et al.²⁴

2. Initial Products and Branching Ratios. The initial species that can be formed from propargyl combination are 15HD, 1245HT, and 12HD5Y. Of these only 15HD and 12HD5Y were observed in quantifiable amounts although a trace of 1245HT was observed for $T_5 < 750$ K and significant quantities of 34DMCB were found in the 720–850 K region where 15HD and 12HD5Y concentrations are constant and no other products are observed. In this temperature regime, 15HD and 12HD5Y account for around 80% of the reaction products. These results are in qualitative agreement with a flow-reactor study by Howe and Fahr³⁰ who used photolysis of three different propargyl precursors to examine the combination reaction between 295 and 623 K and several pressures from 3 to 133 mbar. They found significant quantities of 15HD and a species they assume to be 12HD5Y under all conditions and observed a strong pressure and temperature dependence for 34DMCB. The other initially formed C_6H_6 , 1245HT, was not detected in their study. In contrast, Alkemade and Homann²⁰ observed all three of the initial adducts including 9–17% 1245HT in a flow-tube experiment at 623–673 K and 3–6 mbar. However Alkemade and Homann did not observe any 34DMCB. Furthermore, the theoretical work of Miller and Klippenstein²⁰ also predicts a much lower yield, <5%, of 1245HT than Alkemade and Homann observed experimentally, and they also predict a yield of 34DMCB that is close to the amount of 1245HT observed by Alkemade and Homann. Thus there exists the possibility that the species identified as 1245HT by Alkemade and Homann might have been 34DMCB. However, comparison of the Kovats indices from Alkemade and Homann's study and the current work, Table 3, clearly shows that 1245HT and not 34DMCB was present in Alkemade and Homann's samples. Thus it appears that the 1245HT entrance channel is favored at very low pressures, $P < 6$ mbar, and modest temperatures, $T < 700$ K, but that when the pressure is increased³⁰ the 1245HT then isomerizes quantitatively to 34DMCB. In our earlier other work on 15HD,³² 1245HT was not observed although at 820–950 K 15HD is converted quantitatively to 34DMCB. The reaction occurs via a Cope rearrangement to 1245HT, which then rapidly rearranges to 34DMCB. Clearly an experimental investigation of 1245HT is warranted and has been undertaken in the HPST. A detailed report is currently in preparation,^{47,48} and the preliminary results are reported below.

1245HT was synthesized via a Grignard reaction^{38,39} and formed roughly in a 1:2 ratio with the coproduct 12HD5Y from which it could not be easily separated. GC-MI-FTIR-MS was

SCHEME 2: Truncated Kinetic Model Used for RRKM Analysis of the Thermal Isomerization Initialized from 1245HT^a



^a The number over the arrow represents the critical energy in kcal/mol for the corresponding reaction. All parameters were taken from ref 18 without any modification.

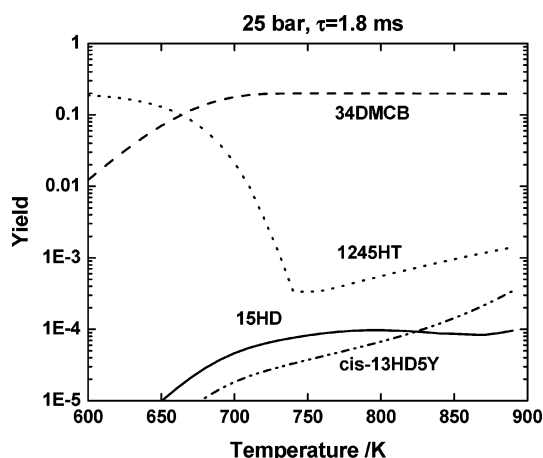


Figure 12. Simulation of the kinetic fate of 1245HT at 25 bar using a truncated kinetic model shown in Scheme 2. The initial 1245HT mole fraction was $[1245HT]_0 = 0.18$.

used to confirm the structures of the products as in earlier work on 15HD isomerization.³¹ A reagent mixture was prepared containing about 5 ppm 1245HT and 10 ppm 12HD5Y, and two HPST experiments were performed at 765 and 712 K. In both cases, <1% of $[1245HT]_0$ remained in the postshock gases and the initial 1245HT was converted to 34DMCB while no change in $[12HD5Y]$ was observed. Additionally a preliminary simulation based on RRKM calculations^{49–51} using a truncated kinetic model, Scheme 2, taken from the Miller and Klippenstein potential energy surface¹⁸ was performed. The results of the simulation are shown in Figure 12 and clearly indicate that, for $T = 700–900$ K, encompassing the temperature regime of the current work where 15HD and 12HD5Y are formed in stable amounts, the 1245HT is converted almost quantitatively to 34DMCB with only traces of 15HD and *cis*-13HD5Y being formed. Thus both the preliminary 1245HT isomerization experiments and the simple modeling work show that in the HPST 1245HT is efficiently converted to 34DMCB at low temperatures. This is in complete accord with our earlier studies on 15HD isomerization³² where quantitative conversion of 15HD into 34DMCB and no 1245HT were observed at 820–950 K. Thus as $[34DMCB] \equiv [1245HT]_0$ the 34DMCB can be used as a surrogate for 1245HT when considering branching ratios for the entrance channels in C_3H_3 combination.

Given the fact that 34DMCB is an accurate marker for the 1245HT entrance channel and that the sole additional products for $T_5 < 800$ K are 15HD and 12HD5Y, then branching ratios for the entrance channels can be obtained from the relative product concentrations. Figure 13 shows an expanded portion of the species profile plots for the 50 and 25 bar experiments for $T_5 < 850$ K. Clearly for $T_5 < 800$ K there is very little

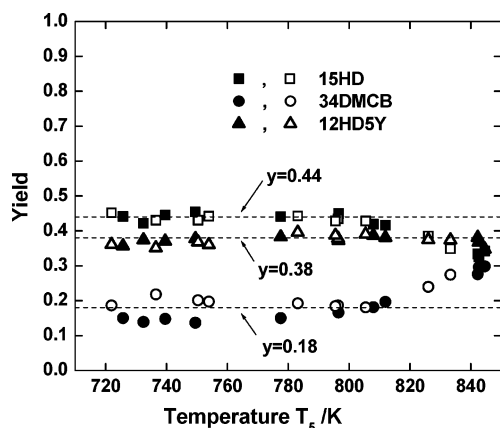


Figure 13. Observed initial branching ratios of propargyl recombination. Closed symbols, 25 bar data; open symbols, 50 bar data. The lines were drawn for visualization.

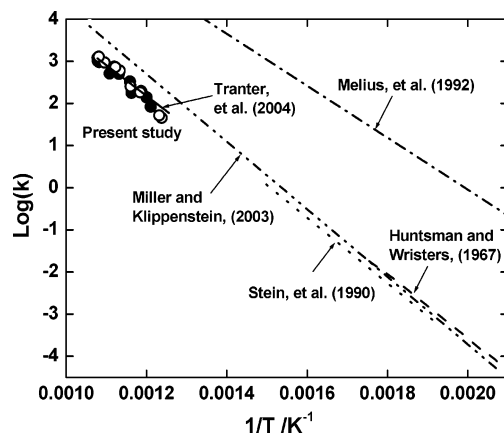


Figure 14. Comparison of the Arrhenius plots for the isomerization of 1,5-hexadiyne. Closed symbols, 25 bar data; open symbols, 50 bar data.

variation in the relative experimental yields of 15HD (44%), 12HD5Y (38%), and 34DMCB (18%). The calculated product distributions by Miller and Klippenstein¹⁸ are 51% 15HD, 30% 12HD5Y, and 18% 1245HT at 650 K and 10 bar and 48% 15HD, 34% 12HD5Y, and 20% 1245HT at 1000 K and 10 bar with all other C_6H_6 species accounting for <1%. Thus there is reasonable agreement between the theoretical predictions and the current experimental work for the 1245HT channel. However the calculations tend to favor the 15HD channel at the expense of the 12HD5Y channel and for $T_5 < 800$ K in the HPST isomerization of 15HD to 12HD5Y is not likely to occur indicating that formation of 12HD5Y is more significant than predicted.

From the experimental species profiles it would appear that the branching ratios are independent of temperature for 720–800 K in the HPST. By assuming that the branching ratios are constant for $T_5 < 950$ K in the HPST experiments, rate coefficients for 15HD isomerization and 12HD5Y isomerization can be estimated from the species profiles. To obtain the rate coefficients, a value for the propargyl combination reaction of $4 \times 10^{-11} \text{ cm}^3 \text{ molecule}^{-1} \text{ s}^{-1}$ was used²⁷ which indicates that, for $[C_3H_3]_0 = 50$ ppm, 2–5 μs are need to consume 99.9% C_3H_3 radicals which is negligible compared to the average residence time of 1.8 ms. The extracted rate coefficients for 15HD isomerization over the temperature range 820–950 K are shown in Figure 14 along with various literature values. The current work is in very good agreement with our earlier studies on 15HD isomerization,³² and the lack of any significant

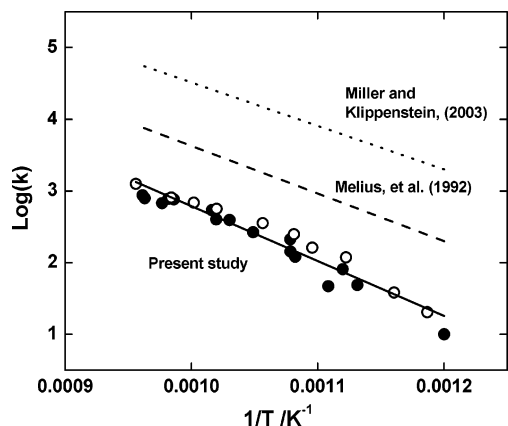


Figure 15. Arrhenius plot of isomerization reaction 12HD5Y \rightarrow 2E13BD. The solid line is the least-squares fit given in text. Closed symbols, 25 bar data; open symbols, 50 bar data.

deviation between the two data sets tends to support the notion that the branching ratios for the C_3H_3 combination entrance channels are temperature independent at least up to 950 K at our working pressures.

Similarly, the rate expression of the 12HD5Y isomerization reaction R8 was deduced to be $k_8 = 10^{10.44} \times \exp(-34.96 \text{ Kcal}/RT)$ in the temperature range 840–1040 K. To the best of our knowledge, this is the first experimental determination of k_8 . Previously Hopf⁵² studied the isomerization of 12HD5Y and found 2E13BD to be the sole product however a rate coefficient for R8 was not obtained. Figure 15 compares k_8 with the two theoretical estimates in the literature.^{13,18} The theoretical calculations are about 1–2 orders of magnitude higher than the experimental determination, a discrepancy far greater than the experimental uncertainty and the margin of errors introduced in our rate deduction. The k_8 value is about 1 order of magnitude lower than that of 15HD isomerization as demonstrated by the faster decay of 15HD than 12HD5Y in Figures 4a and 5a.



3. Secondary Products. In addition to the three primary products and the trace of 1245HT, several secondary products are formed in C_3H_3 combination reactions by isomerization of the primary products. The secondary products include *cis*- and *trans*-13HD5Y, fulvene, benzene, and 2E13BD. In comparison with our earlier work on 15HD, performed to explore the isomerization reactions of C_3H_3 combination products, the major differences are that nearly 60% more 13HD5Y (total for both isomers) is formed in the 15HD work when considering relative mole fractions in the two sets of experiments (see Figure 16). Considerably more 2E13BD is present in the current C_3H_3 work. The higher 2E13BD concentration is directly attributable to the fact that it is formed exclusively from 12HD5Y which accounts for 38% of the initial recombination products in the C_3H_3 experiments. The current study of C_3H_3 combination is the first time that 2E13BD has been observed and quantified, although given the peak distributions for unidentified C_6H_6 species in Scherer et al.'s work,²⁴ it is likely that the species is present there as well. Under the conditions of Alkemade and Homann's study, the temperature was probably too low for isomerization of 12HD5Y to 2E13BD and a preliminary study of 12HD5Y isomerization in the HPST indicates this assumption is correct.

In the C_3H_3 combination experiments, $[13HD5Y]_{\text{total}}$ reaches a maximum at 1060 K of 14%, whereas in the 15HD experiments $[13HD5Y]_{\text{totalmax}} = 8\%$ and occurs at the same temper-

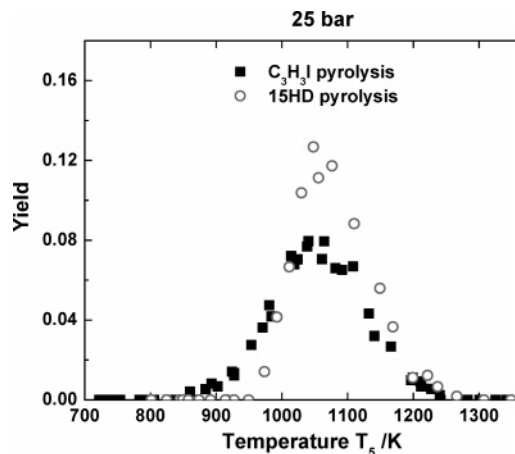


Figure 16. Comparison of 13HD5Y production in C_3H_3I pyrolysis (■) and in 15HD pyrolysis (○) at 25 bar.

ature, Figure 16. This difference can be explained by considering the branching ratios in the C_3H_3I experiments and bearing in mind the reaction paths shown in Scheme 1 that indicate that 13HD5Y is formed from 1245HT. The experimentally determined relative ratio ($0.14/0.08 = 1.625$) is a precise match to the one according to entry branching ratios ($1.0/(0.44 + 0.18) = 1.610$). (Note the numerator is 1.0 because in 15HD pyrolysis all reactant can form 13HD5Y. The denominator is $(0.44 + 0.18)$ because in propargyl recombination the 0.38 portion of 12HD5Y does not have the chance forming 13HD5Y). Thus all of the 13HD5Y is formed both indirectly from 15HD via isomerizing 1245HT and also directly from 1245HT, and 12HD5Y plays no role in the formation of 13HD5Y for temperatures below 1060 K.

Bearing the differences in $[13HD5Y]$ and $[2E13BD]$ in mind, the distribution of secondary products and their temperature-dependent behavior is completely consistent with the arguments advanced in the earlier 15HD work³² and the reader is referred to this publication for a detailed discussion of the comparison of the isomer distributions with prior experimental work and the Miller and Klippenstein potential energy surface.

Conclusions

An extensive experimental study of the self-recombination of propargyl radicals has been performed at two reaction pressures of 25 and 50 bar with temperature ranging from 720 to 1350 K. Propargyl iodide was synthesized and used as radical source. The HI elimination channel and the minor presence of iodoallene were experimentally determined to have no effect on the isomeric C_6H_6 product distributions. Nine C_6H_6 isomers including trace amounts of 1245HT were observed for $T_5 < 750$ K. The entry branching ratios are determined as 44% 15HD, 38% 12HD5Y, and 18% 1245HT, which is efficiently converted to 34DMCB at our experimental conditions. After the initial recombination step, various isomeric products are formed by thermal isomerization, with the distribution primarily depending on reaction temperature. The isomerization route forming benzene from 12HD5Y occurs at a higher temperature than that from 15HD and 1245HT. The current experiment is to a large degree consistent with the theoretical work of Miller and Klippenstein. However, the calculation overpredicts considerably the isomerization rate of 12HD5Y \rightarrow 2E13BD, which implies the necessity of reevaluation of some wells/channels in the current potential to allow 12HD5Y to be collisionally stabilized at moderate temperature. An experimental study on 12HD5Y is also warranted to resolve the discrepancy.

The detailed species concentration profiles measured in the current work (the direct recombination of propargyl radicals) and in the previous 15HD work provide the necessary information for the development and validation of a $C_3H_3 + C_3H_3$ submechanism that can be included in detailed kinetic models for better descriptions of benzene formation from propargyl radicals. To achieve such a submechanism, a comprehensive numeric/modeling study has been conducted in this laboratory. The results will be published separately.⁵³

Acknowledgment. This work was supported by the United States National Science Foundation under Contract CTS 0109053. Dr. Ken Anderson at Southern Illinois University is greatly acknowledged for the identification of 1245HT.

Supporting Information Available: Tables of experimental data containing reaction conditions and species distributions. This material is available free of charge via the Internet at <http://pubs.acs.org>.

References and Notes

- (1) Miller, J. A. *Faraday Discuss.* **2001**, *119*, 461.
- (2) Miller, J. A. *Proc. Combust. Inst.* **1996**, *20*, 461.
- (3) Richter, H.; Howard, J. B. *Prog. Energy Combust. Sci.* **2000**, *26*, 565.
- (4) D'Anna, A.; Violi, A.; D'Allesio, A. *Combust. Flame* **2000**, *121*, 418.
- (5) Miller, J. A.; Kee, R. J.; Westbrook, C. K. *Annu. Rev. Phys. Chem.* **1990**, *41*, 345.
- (6) Lindstedt, P. *Proc. Combust. Inst.* **1998**, *27*, 269.
- (7) Lindstedt, P.; Skevis, G. *Proc. Combust. Inst.* **1996**, *26*, 693.
- (8) Pope, C. J.; Miller, J. A. *Proc. Combust. Inst.* **2000**, *28*, 1519.
- (9) Appel, J.; Bockhorn, H.; Frenklach, M. *Combust. Flame* **2000**, *121*, 122.
- (10) Richter, H.; Howard, J. B. *Phys. Chem. Chem. Phys.* **2002**, *4*, 2034.
- (11) Thomas S. D.; Communal F.; Westmoreland, P. R. *ACS Div. Fuel Chem.* **1991**, 1449.
- (12) Miller, J. A.; Melius, C. F. *Combust. Flame* **1992**, *91*, 21.
- (13) Melius, C. F.; Miller, J. A.; Evleth, E. M. *Proc. Combust. Inst.* **1992**, *24*, 621.
- (14) Miller, J. A.; Klippenstein S. J. *J. Phys. Chem. A* **2001**, *105*, 7254.
- (15) Klippenstein, S. J.; Miller, J. A. *J. Phys. Chem. A* **2002**, *106*, 9267.
- (16) Dean, A. M. *J. Phys. Chem.* **1985**, *89*, 4600.
- (17) Carstensen, H.-H.; Dean, A. M., private communication.
- (18) Miller, J. A.; Klippenstein S. J. *J. Phys. Chem. A* **2003**, *107*, 7783.
- (19) Stein, S. E.; Walker, J. A.; Suryan, M.; Fahr, A. *Proc. Combust. Inst.* **1990**, *23*, 85.
- (20) Alkemade, U.; Homann, K. H. *Z. Phys. Chem.* **1989**, *161*, 19.
- (21) Morter, C. L.; Farhat, S. K.; Adamson, J. D.; Glass, G. P.; Curl, R. F. *J. Phys. Chem.* **1994**, *98*, 7029.
- (22) Atkinson, D. B.; Hudgens, J. W. *J. Phys. Chem. A* **1999**, *103*, 4242.
- (23) Fahr, A.; Nayak, A. *Int. J. Chem. Kinet.* **2000**, *32*, 118.
- (24) Scherer, S.; Just, T.; Frank, P. *Proc. Combust. Inst.* **2000**, *28*, 1511.
- (25) DeSain, J. D.; Taatjes, C. A. *J. Phys. Chem. A* **2003**, *107*, 4843.
- (26) Shafir, E. V.; Slagle, I. R.; Knyazev, V. D. *J. Phys. Chem. A* **2003**, *107*, 8893.
- (27) Giri, B. R.; Hippler, H.; Olzmann, M.; Unterreiner, A. N. *Phys. Chem. Chem. Phys.* **2003**, *5*, 4641.
- (28) Fernandes, R. X.; Hippler, H.; Olzmann, M. *Proc. Combust. Inst.* **2004**, *30*, in press.
- (29) Rasmussen, C. L.; Skjøth-Rasmussen, M. S.; Jensen, A. D.; Glarborg, P. *Proc. Combust. Inst.* **2004**, *30*, in press.
- (30) Howe, P. T.; Fahr, A. *J. Phys. Chem. A* **2003**, *107*, 9603.
- (31) Anderson, K. B.; Tranter, R. S.; Tang, W.; Brezinsky, K.; Harding, L. B. *J. Phys. Chem. A* **2004**, *108*, 3403.
- (32) Tranter, R. S.; Tang, W.; Anderson, K. B.; Brezinsky, K. *J. Phys. Chem. A* **2004**, *108*, 3406.
- (33) Tranter R. S.; Fulle D.; Brezinsky K. *Rev. Sci. Instr.* **2001**, *72*, 3046.
- (34) Tranter, R. S.; Sivaramakrishnan, R.; Srinivasan, R.; Brezinsky, K. *Int. J. Chem. Kin.* **2001**, *33*, 722.
- (35) Hidaka, Y.; Shiba, S.; Takuma, H.; Suga, M. *Int. J. Chem. Kin.* **1985**, *17*, 441.
- (36) Davidson D. F.; Hanson R. K. *Isr. J. Chem.* **1996**, *36*, 321.
- (37) Finkelstein, H. *Chem. Ber.* **1910**, *43*, 1528.
- (38) Hopf, H. *Angew. Chem. Intl. Ed.* **1970**, *9*, 732.
- (39) Hopf, H.; Bohm, I.; Kleinschroth, M. *J. Org. Synth.*, CV 7, 485. Also at <http://www.orgsyn.org/orgsyn/orgsyn/prepContent.asp?prep=cv7p0485>, 2005.
- (40) Kern, R. D.; Chen, H.; Kiefer, J. H.; Mudipalli, P. S. *Combust. Flame* **1995**, *100*, 177.
- (41) Lee, Y.-R.; Lin, S.-M. *J. Chem. Phys.* **1998**, *108*, 134.
- (42) Kawasaki, M.; Kasatani, K.; Sato, H. *Chem. Phys.* **1984**, *88*, 135.
- (43) Browning, P. W.; Kitchen, D. C.; Arendt, M. F.; Butler L. J. *J. Phys. Chem.* **1996**, *100*, 7765.
- (44) Miller, J. A.; Klippenstein S. J. *J. Phys. Chem. A* **2003**, *107*, 2680.
- (45) Kumaran, S. S.; Lim, K. P.; Michael, J. V.; Tilson, J. L.; Suslensky, A.; Lifshitz, A. *Isr. J. Chem.* **1996**, *36*, 223.
- (46) Herzler, J.; Frank, P. *Springer Ser. Chem. Phys.* **1994**, *59*, 11.
- (47) Miller, C. M. S. thesis, University of Illinois at Chicago, 2005.
- (48) Manuscript in preparation.
- (49) Troe, J. *J. Chem. Phys.* **1977**, *66*, 4745.
- (50) Troe, J. *J. Chem. Phys.* **1977**, *66*, 4758.
- (51) Holbrook, K. A.; Piling, M. J.; Robertson, S. H. *Unimolecular Reactions*, 2nd ed.; John Wiley & Sons: 1996.
- (52) Hopf, H. *Angew. Chem.* **1970**, *82*, 703.
- (53) Tang, W.; Tranter, R. S.; Brezinsky, K. *J. Phys. Chem. A*, submitted for publication.